

# The influence of initial stresses on energy release rate and total electro-mechanical potential energy for penny-shaped interface cracks in PZT/Elastic/PZT sandwich circular plate-disc

Surkay D. Akbarov<sup>\*1,2</sup>, Fazile I. Cafarova<sup>3</sup> and Nazmiye Yahnioglu<sup>4</sup>

<sup>1</sup>Department of Mechanical Engineering, Yildiz Technical University 34349, Besiktas, Istanbul, Turkey

<sup>2</sup>Institute of mathematics and Mechanics of the National Academy of Sciences of Azerbaijan, AZ1141, Baku, Azerbaijan

<sup>3</sup>Genje State University, Genje, Azerbaijan

<sup>4</sup>Department of Mathematical Engineering, Yildiz Technical University, Davutpasa Campus, 34220, Esenler, Istanbul, Turkey

(Received March 13, 2018, Revised July 20, 2018, Accepted July 24, 2018)

**Abstract.** This paper studies the energies and energy release rate (ERR) for the initially rotationally symmetric compressed (or stretched) in the inward (outward) radial direction of the PZT/Elastic/PZT sandwich circular plate with interface penny-shaped cracks. The investigations are made by utilizing the so-called three-dimensional linearized field equations and relations of electro-elasticity for piezoelectric materials. The quantities related to the initial stress state are determined within the scope of the classical linear theory of piezoelectricity. Mathematical formulation of the corresponding problem and determination of the quantities related to the stress-strain state which appear as a result of the action of the uniformly normal additional opening forces acting on the penny-shaped crack's edges are made within the scope of the aforementioned three-dimensional linearized field equations solution which is obtained with the use of the FEM modelling. Numerical results of the energies and ERR and the influence of the problem parameters on these quantities are presented and discussed for the PZT-5H/Al/PZT-5H, PZT-4/Al/PZT-4, BaTiO<sub>3</sub>/Al/BaTiO<sub>3</sub> and PZT-5H/StPZT-5H sandwich plates. In particular, it is established that the magnitude of the influence of the piezoelectricity and initial loading on the ERR increases with crack radius length.

**Keywords:** electro-mechanical energy; energy release rate; piezoelectric material; penny-shaped interface crack; sandwich circular plate

## 1. Introduction

In many modern branches of engineering, piezoelectric (PZT) ceramics have great application in micro- and macro-electro-mechanical systems and smart composites. At the same time, PZT materials are widely used as sensors or actuators under which the layers made from these are glued onto the face surface of the basic materials. Moreover, under manufacturing of smart composites, there are many cases under which the layers made of PZT are alternated with layers made from elastic materials. Safety of the aforementioned systems depends not only on preventing a fracture of each layer's material separately but also on preventing an adhesion strength (or fracture) between the PZT and pure elastic layers. Note that the adhesion strength is weakened significantly with debonding zones which commonly arise between the layers during the assembly process of these layers or in consequence of various external factors. It is evident that in the corresponding external loading cases the noted debonding zones may

cause highly inhomogeneous and concentrated stresses around these zones and hence, decrease the strength and service life of these expensive electro-mechanical systems. For controlling of the debonding interface zones on the electro-mechanical behavior of the PZT/Elastic systems, it is necessary to make fundamental studies on this influence based on the modern theories of piezoelectricity and elasticity. Note that in many cases under these studies, the debonding zones are modeled as interface cracks, the electro-mechanical behavior of which depends also on the external loading direction. So that, in the case where the external mechanical loading acts in a direction which is perpendicular to the cracks' edges, these cracks may cause interface fractures of the layers. However, in the cases where the external loading acts in a direction which is parallel to the cracks' edges, these cracks may cause buckling delamination around the cracks (see, for instance, Akbarov (2013), Akbarov and Yahnioglu (2013) and other ones listed therein). Moreover, the electro-mechanical behavior of the cracks also significantly depends on their geometries. For instance, in the so-called three-dimensional crack problems, penny-shaped, elliptical and other similar types of models are used. Thus, according to the foregoing brief discussion, it can be concluded that the mathematical modelling and theoretical investigations related to the electro-mechanical interface crack problems, to which the present paper is also concerned, have great significance in the fundamental and application sense.

\*Corresponding author, Research Professor

E-mail: akbarov@yildiz.edu.tr

<sup>a</sup> Ph.D.

E-mail: nazmiye@yildiz.edu.tr

<sup>b</sup> Ph.D. Student

E-mail: fazile.cafarova@mail.ru

For estimation of the development of the investigation made in the present work and its significance, amongst others, we consider a brief review of related investigations and, according to the subject of the paper, analyze mainly the works studying the problems regarding penny-shaped cracks in piezoelectric materials.

The first attempt for the study of the fracture problem related to the penny-shaped crack embedded in a piezoelectric material is made in the paper by Kudryatsev *et al.* (1975) in which a special solution of the stress and displacement fields is obtained. Under mathematical formulation of the problem, the so-called permeable condition on the crack edges is considered, according to which, it is assumed that the electrical potential and the normal components of the electrical displacements are continuous across the crack edge surfaces. In this case, the penny-shaped crack is treated as a mathematical cut filled with air. The same type of conditions on the crack's edge are also used in the papers by Parton (1976), Yang (2004) and other ones listed therein. More detailed analyses of the various types of conditions on the crack edges in the piezoelectric materials are discussed in the papers by McMeeking and Landis (2008) and Fent *et al.* (2009). Moreover, in the paper by Yang (2004), the penny-shaped crack problem for the mode I under far-field uniform mechanical and electrical loading and under mechanical loading on the faces of the crack is studied within the scope of the linear piezoelectric fracture mechanics by employing the Hankel integral transformation method. For the cases under consideration, corresponding expressions for the Stress Intensity Factor (SIF) and for the electric displacement intensity factor (EDIF) are obtained. At the same time, the corresponding analytical expressions are determined for the Energy Release Rate (ERR).

The paper by Li and Lee (2012) studies an axisymmetric penny-shaped crack problem for the infinite piezoelectric layer in the case where the crack is in the middle plane of the layer. On the crack's edge surfaces the impermeable boundary condition model is used. According to this model, it is assumed that the electric displacements on the crack's edge surfaces are equal to zero. Moreover, in the paper by Li and Lee (2012), a new method is developed for determination of the corresponding fundamental solutions and by employing this method numerical results related to the ERR are presented and discussed.

The axisymmetric penny-shaped crack problem for the infinite piezoelectric layer is also considered in the paper by Zhong (2012) in the case where the crack is on the plane which is parallel to the face planes of the layer. Moreover, in this paper on the crack edges, the energetically consistent boundary condition model proposed in the paper by Landis (2004) is used. The solution of the corresponding boundary value problem for the mode I is made by use of the Hankel integral transformation method. Numerical results on the ERR and SIF are presented and discussed.

The energetically consistent boundary condition model on the crack's edges is also used in the paper by Eskandari *et al.* (2010) for investigation of the axisymmetric annular crack problem in the infinite piezoelectric material. The far-field electrical and mechanical loading case for the mode I

is considered. The analytical solution method, based also on the Hankel integral transformation, is employed. Numerical results on the ERR, electric displacement etc. are presented and discussed.

The annular interface crack problem between dissimilar piezoelectric layers for the mode I is considered in the paper by Li *et al.* (2011) in which an impermeable boundary condition on the crack's edge surface is assumed. As in the previous papers, the Hankel integral transformation and the integral equation method are employed for solution of the corresponding boundary value problem. Numerical results on the ERR of the inner and outer crack tips are presented and discussed for various problem parameters.

The paper by Nanta *et al.* (2003) deals with the study of the penny-shaped crack in the piezoelectric infinite cylinder under mode I loading. The permeable boundary condition model on the crack's edge surface is considered. The aforementioned well-known integral transformation solution method is employed and numerical results on the ERR, SIF and energy density factor are obtained for the far-field mechanical and electrical loading cases under various values of the problem parameters. Note that these results are obtained not only for the permeable, but also for the impermeable boundary condition model on the crack's edge. Consequently, as a result of the comparison of these results, the effect of the permeability condition on the values of the fracture parameters of the penny-shaped crack in a piezoelectric material is shown.

The fracture problem for a penny-shaped interface crack between a functionally graded piezoelectric layer and a homogeneous piezoelectric layer is investigated in the paper by Li *et al.* (2009). It is assumed that on the crack's edges the impermeable boundary condition is satisfied and on the face planes of the bi-layered plate the uniformly distributed normal stretching forces and electrical displacements act simultaneously. Moreover, the mechanical and electrical properties of the functionally graded material are assumed to vary continuously along the layer thickness direction and this assumption simplifies significantly the solution procedures and allows the analytical solution of the corresponding boundary value problem to be obtained. The traditional solution method indicated above is also used in this work and numerical results on the SIF and ERR are obtained and discussed for various values of the problem parameters.

In all the works reviewed above it is assumed that the penny-shaped crack is embedded completely in a piezoelectric material and therefore formulation of the permeable, impermeable, energetically consistent, semi-consistent and other types of conditions for the electrical quantities across the crack's edge surfaces, becomes necessary. However, in the cases where the penny-shaped crack is in the interface between piezoelectric and elastic mediums such conditions do not have any meaning. Therefore, in later cases on the crack's edge face which relate to the piezoelectric medium, the ordinary "electrically-open" (or "open-circuit") and "electrically-shortened" (or "short-circuit") conditions are given. Note that the "electrically-open" (or "open-circuit") condition coincides with the aforementioned impermeable condition.

In connection with this, according to the authors' knowledge, we note that the first attempt to study the problem related to the interface penny-shaped crack between the piezoelectric layer and half-space is made in the paper by Ren *et al.* (2014). This study is carried out for the opening mode in the case where on the crack face, which is in the piezoelectric layer, the "open-circuit" condition is satisfied. The corresponding problem, as in the foregoing papers, is solved with utilizing the Hankel transform and singular integral equation methods and according to this analytical solution, numerical results on the ERR and SIF are obtained and discussed.

With this we restrict ourselves to consideration of the review of the investigations related to the penny-shaped crack in piezoelectric materials. Note that under this review we have considered mainly the works which have been carried out during the last 10 years. A review of the related works carried out on earlier dates can be found in the above reviewed papers. Moreover, note that a more detailed review regarding other investigations can be found in the papers by Kuna (2006) and Kuna (2010).

Thus, it follows from the foregoing review that all the investigations carried out for the penny-shaped cracks in piezoelectric materials and in the interface between piezoelectric and elastic materials have been made within the scope of the linear piezoelectric fracture mechanics and within the scope of the assumptions that the layers' dimensions are infinite in the plane on which this crack lies. It is known that the linear theory of piezoelectricity cannot take into consideration the influence of the homogeneous normal stresses acting in the directions which are parallel to the crack's edge planes on the fracture parameters such as SIF, ERR etc. Note that the approach for solution of the corresponding pure elastic problems is first proposed by Guz and the corresponding results of this author and his students are detailed in the monograph by Guz (1981). Some elements of this approach are also given in the other monograph by Guz (1999). Note that this approach is based on the so-called three-dimensional linearized theory of elasticity, the field equations and relations of which are obtained through the linearization of the corresponding geometrically non-linear field equations and relations. Under these linearized procedures, the stresses acting along the laying direction of the cracks' edges are assumed as initial ones and the stress-strain fields caused by the additional forces acting on the cracks' edge surfaces are determined through the linearized equations, the coefficients of which contain the initial stresses. Namely, this statement allows us to take into consideration the influence of the initial stresses on the SIF and ERR at the cracks' tips.

The corresponding linearization procedures are also made for the field equations and relations of the theory of piezoelectricity (see, for instance, the monograph by Yang (2005) and other ones listed therein). However, up to now the study of the influence of the initial stress on the SIF and ERR at the crack's tips which are in the piezoelectric materials or in the interface between the piezoelectric and elastic medium is almost completely absent. To the best knowledge of the authors, the first attempt in this field is

made in the paper by Akbarov and Yahnioğlu (2016), in which in the plane strain state, the influence of the initial stresses on the total electro-mechanical potential energy and ERR at the cracks' tips located on the interface planes of the sandwich plate-strip with piezoelectric face and elastic core layers, is studied. Note that the corresponding buckling delamination problem is studied in the paper by Akbarov and Yahnioğlu (2013). Moreover, in the paper by Akbarov and Turan (2009) the corresponding crack problem in an initially stressed orthotropic elastic plate-strip is examined.

Taking the foregoing statement and the theoretical application significance of the related investigation into consideration, in the present paper we attempt to develop the investigations started in the paper by Akbarov and Yahnioğlu (2013) to the penny-shaped interface cracks which are located on the interface of the circular sandwich plate with piezoelectric face and elastic middle layers. Under these investigations, it is assumed that in the first stage on the lateral boundary of the sandwich plate disc, the uniformly distributed normal compressing (or stretching) forces act in the inward (outward) radial direction and these forces at a certain distance from the lateral boundary cause corresponding homogeneous stresses in the layers. In the second stage it is assumed that on the edges of the penny-shaped interface cracks, the additional opening normal forces are applied. It is required to determine the influence of the homogeneous initial stresses which appear in the first stage on the ERR caused by the additional normal opening forces acting on the cracks' edge surfaces in the second stage. Note that the corresponding buckling delamination problem is considered in the paper by Cafarova *et al.* (2017).

## 2. Formulation of the problem

We consider a circular sandwich plate with geometry illustrated in Fig. 1 and assume that the thicknesses and materials of the face layers are the same and piezoelectric, and the material of the middle (core) layer is an elastic one. Moreover, assume that between the core and face layers there are penny-shaped cracks whose locations are also illustrated in Fig. 1.

Associate with the lower face plane of the plate the cylindrical coordinate system  $Or\theta z$  (Fig. 1), according to which, the plate occupies the region  $\{0 \leq r \leq \ell/2; 0 \leq \theta \leq 2\pi; 0 \leq z \leq h\}$  ( $h = 2h_F + h_C$ ) and

the penny-shaped cracks occur in  $\{z = h_F \pm 0; 0 \leq r \leq \ell_0/2\}$  and in  $\{z = h_C + h_F \pm 0; 0 \leq r \leq \ell_0/2\}$ .

Thus, within this framework, we suppose that at first, the plate is loaded by uniformly distributed rotationally symmetric normal forces with intensity  $q$  (Fig. 1(b)) acting on the lateral surface of the circular plate-disc. The electro-mechanical state caused with this loading is called the initial state. After this initial state appears, i.e., in the second stage, we assume that the cracks' edges are loaded by additional uniformly distributed normal opening forces

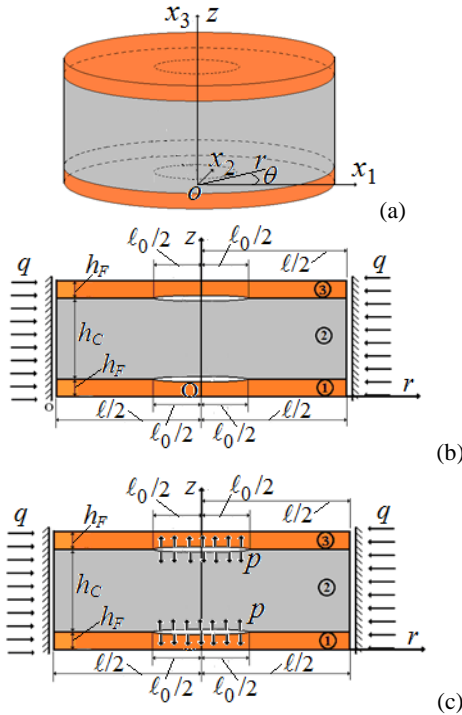


Fig. 1 The geometry of the plate-disc and interface penny-shaped cracks: (a) the whole sandwich plate-disc, (b) the radial section of the plate – disc and its loading in the initial state and (c) the radial section of the plate-disc with additional loading acting on the crack’s edges

with intensity  $p$  (Fig. 1(c)) and assume that the magnitude of  $p$  is less significant than that of  $q$ .

Now we consider formulation of the problems for determination of the electro-mechanical quantities related to the first (initial) and second stages. As we are considering the rotationally axisymmetric deformation case, therefore under the aforementioned formulation we will use the corresponding field equations related to this case. Moreover, below we will denote the values related to the upper and lower face layers by upper indices (3) and (1), respectively, whereas the values related to the core layer are denoted by (2). The values related to the first (initial) state will be distinguished from those related to the second stage with the additional upper index 0.

2.1 For the first stage

We assume that in the first stage, the electro-mechanical state in the sandwich plate under consideration appears within the scope of the linear theory of piezoelectricity for the face layers and the linear theory of elasticity for the core layer. According to the monograph by Yang (2005), the field equations are:

Equilibrium and electrostatic equations

$$\frac{\partial \sigma_{rr}^{(j)0}}{\partial r} + \frac{\partial \sigma_{rz}^{(j)0}}{\partial z} + \frac{1}{r}(\sigma_{rr}^{(j)0} - \sigma_{\theta\theta}^{(j)0}) = 0 \quad (1)$$

$$\frac{\partial \sigma_{rz}^{(j)0}}{\partial r} + \frac{\partial \sigma_{zz}^{(j)0}}{\partial z} + \frac{1}{r} \sigma_{rz}^{(j)0} = 0, \quad j=1,2,3$$

$$\frac{\partial D_r^{(k)0}}{\partial r} + \frac{1}{r} D_r^{(k)0} + \frac{\partial D_z^{(k)0}}{\partial z} = 0, \quad k=1,3$$

The electro-mechanical constitutive relations for piezoelectric materials

$$\sigma_{rr}^{(k)0} = c_{1111}^{(k)} s_{rr}^{(k)0} + c_{1122}^{(k)} s_{\theta\theta}^{(k)0} + c_{1133}^{(k)} s_{zz}^{(k)0} -$$

$$e_{111}^{(k)} E_r^{(k)0} - e_{311}^{(k)} E_z^{(k)0}$$

$$\sigma_{\theta\theta}^{(k)0} = c_{2211}^{(k)} s_{rr}^{(k)0} + c_{2222}^{(k)} s_{\theta\theta}^{(k)0} + c_{2233}^{(k)} s_{zz}^{(k)0} -$$

$$e_{122}^{(k)} E_r^{(k)0} - e_{322}^{(k)} E_z^{(k)0}$$

$$\sigma_{zz}^{(k)0} = c_{3311}^{(k)} s_{rr}^{(k)0} + c_{3322}^{(k)} s_{\theta\theta}^{(k)0} + c_{3333}^{(k)} s_{zz}^{(k)0} -$$

$$e_{133}^{(k)} E_r^{(k)0} - e_{333}^{(k)} E_z^{(k)0}$$

$$\sigma_{rz}^{(k)0} = c_{1311}^{(k)} s_{rz}^{(k)0} - e_{113}^{(k)} E_r^{(k)0} - e_{313}^{(k)} E_z^{(k)0}$$

$$D_r^{(k)0} = e_{111}^{(k)} s_{rr}^{(k)0} + e_{122}^{(k)} s_{\theta\theta}^{(k)0} + e_{133}^{(k)} s_{zz}^{(k)0} +$$

$$\varepsilon_{11}^{(k)} E_r^{(k)0} + \varepsilon_{13}^{(k)} E_z^{(k)0}$$

$$D_z^{(k)0} = e_{311}^{(k)} s_{rr}^{(k)0} + e_{322}^{(k)} s_{\theta\theta}^{(k)0} + e_{333}^{(k)} s_{zz}^{(k)0} +$$

$$\varepsilon_{31}^{(k)} E_r^{(k)0} + \varepsilon_{33}^{(k)} E_z^{(k)0}$$

$$E_r^{(k)0} = -\frac{\partial \phi^{(k)0}}{\partial r}, \quad E_z^{(k)0} = -\frac{\partial \phi^{(k)0}}{\partial z}$$

$$\sigma_{rr}^{(2)0} = \lambda^{(2)} s^{(2)0} + 2\mu^{(2)} s_{rr}^{(2)0} \quad (2)$$

$$\sigma_{\theta\theta}^{(2)0} = \lambda^{(2)} s^{(2)0} + 2\mu^{(2)} s_{\theta\theta}^{(2)0}$$

$$\sigma_{zz}^{(2)0} = \lambda^{(2)} s^{(2)0} + 2\mu^{(2)} s_{zz}^{(2)0}$$

$$\sigma_{rz}^{(2)0} = 2\mu^{(2)} s_{rz}^{(2)0}$$

$$s^{(2)0} = s_{rr}^{(2)0} + s_{\theta\theta}^{(2)0} + s_{zz}^{(2)0}, k=1,3 \quad (3)$$

Strain-displacement relations

$$s_{rr}^{(j)0} = \frac{\partial u_r^{(j)0}}{\partial r}, s_{\theta\theta}^{(j)0} = \frac{u_r^{(j)0}}{r}, s_{zz}^{(j)0} = \frac{\partial u_z^{(j)0}}{\partial z} \quad (4)$$

$$s_{rz}^{(j)0} = \frac{1}{2} \left( \frac{\partial u_r^{(j)0}}{\partial z} + \frac{\partial u_z^{(j)0}}{\partial r} \right), j=1,2,3$$

In (1)-(4) the following notation is used:  $\sigma_{rr}^{(j)}, \dots, \sigma_{rz}^{(j)}$  and  $s_{rr}^{(j)}, \dots, s_{rz}^{(j)}$  are the components of the stress and strain tensors, respectively,  $u_r^{(j)}$  and  $u_z^{(j)}$  are the components of the displacement vector,  $D_r^{(k)}$  and  $D_z^{(k)}$  are the components of the electrical displacement vector,  $E_r^{(k)}$  and  $E_z^{(k)}$  are the components of the electrical field vector,  $\phi^{(k)0}$  is the electric potential,  $\lambda^{(2)}$  and  $\mu^{(2)}$  are Lamé constants of the core layer material, and  $c_{ijkl}^{(k)}, e_{nij}^{(k)}$  and  $\varepsilon_{ij}^{(k)}$  ( $k=1,2,3$ ) are the elastic, piezoelectric and dielectric constants, respectively.

Note that the piezoelectric material exhibits the characteristics of orthotropic materials with the corresponding elastic symmetry axes and becomes electrically polarized under mechanical loads or mechanical deformation placed in an electrical field. According to the monograph by Yang (2005) and other related references, the polled direction of the piezoelectric material will change according to the position of the material constants in the constitutive relations in (2). In the present paper, under numerical calculations, it is assumed that the  $Oz$  axis direction is the polarized direction. Moreover, we introduce the following notation.

$$c_{1111}^{(k)} = c_{11}^{(k)}, c_{2211}^{(k)} = c_{1122}^{(k)} = c_{12}^{(k)}, c_{3311}^{(k)} = c_{1133}^{(k)} = c_{13}^{(k)}$$

$$c_{2222}^{(k)} = c_{22}^{(k)}, c_{3322}^{(k)} = c_{2233}^{(k)} = c_{23}^{(k)}, c_{3333}^{(k)} = c_{33}^{(k)}$$

$$c_{1313}^{(k)} = c_{55}^{(k)}, e_{111}^{(k)} = e_{11}^{(k)}, e_{311}^{(k)} = e_{31}^{(k)}, e_{122}^{(k)} = e_{12}^{(k)} \quad (5)$$

$$e_{322}^{(k)} = e_{32}^{(k)}, e_{133}^{(k)} = e_{13}^{(k)}, e_{333}^{(k)} = e_{33}^{(k)}$$

$$e_{313}^{(k)} = e_{35}^{(k)}, e_{113}^{(k)} = e_{15}^{(k)}$$

Thus, Eqs. (1)-(5) complete the field equations for the case under consideration. Now we consider the formulation of the boundary and contact conditions:

Boundary conditions on the cracks' edges

$$\sigma_{zr}^{(3)0} \Big|_{z=h_F+h_C+0} = 0, \sigma_{zz}^{(3)0} \Big|_{z=h_F+h_C+0} = 0$$

$$\sigma_{zr}^{(2)0} \Big|_{z=h_F+h_C-0} = 0, \sigma_{zz}^{(2)0} \Big|_{z=h_F+h_C-0} = 0 \quad (6)$$

$$\sigma_{zr}^{(2)0} \Big|_{z=h_F+0} = 0, \sigma_{zz}^{(2)0} \Big|_{z=h_F+0} = 0$$

$$\sigma_{zr}^{(1)0} \Big|_{z=h_F-0} = 0, \sigma_{zz}^{(1)0} \Big|_{z=h_F-0} = 0$$

$$D_z^{(3)0} \Big|_{z=h_F+h_C+0} = 0, D_z^{(1)0} \Big|_{z=h_F-0} = 0$$

for  $0 \leq r \leq \ell_0/2$

Contact conditions between the layers in the areas which are out of the cracks

$$\sigma_{zz}^{(3)0} \Big|_{z=h_F+h_C} = \sigma_{zz}^{(2)0} \Big|_{z=h_F+h_C}$$

$$\sigma_{zr}^{(3)0} \Big|_{z=h_F+h_C} = \sigma_{zr}^{(2)0} \Big|_{z=h_F+h_C}$$

$$u_z^{(3)0} \Big|_{z=h_F+h_C} = u_z^{(2)0} \Big|_{z=h_F+h_C}$$

$$u_r^{(3)0} \Big|_{z=h_F+h_C} = u_r^{(2)0} \Big|_{z=h_F+h_C}, \sigma_{zz}^{(2)0} \Big|_{z=h_F} = \sigma_{zz}^{(1)0} \Big|_{z=h_F} \quad (7)$$

$$\sigma_{zr}^{(2)0} \Big|_{z=h_F} = \sigma_{zr}^{(1)0} \Big|_{z=h_F}, u_z^{(2)0} \Big|_{z=h_F} = u_z^{(1)0} \Big|_{z=h_F}$$

$$u_r^{(2)0} \Big|_{z=h_F} = u_r^{(1)0} \Big|_{z=h_F}, D_z^{(3)0} \Big|_{z=h_F+h_C} = 0$$

$$D_z^{(1)0} \Big|_{z=h_F} = 0 \text{ for } \ell_0/2 \leq r \leq \ell/2$$

Boundary conditions on the face planes of the plate

$$\sigma_{zz}^{(3)0} \Big|_{z=2h_F+h_C} = 0, \sigma_{zr}^{(3)0} \Big|_{z=2h_F+h_C} = 0, \sigma_{zz}^{(1)0} \Big|_{z=0} = 0$$

$$\sigma_{zr}^{(1)0} \Big|_{z=0} = 0, D_z^{(3)0} \Big|_{z=2h_F+h_C} = 0, D_z^{(1)0} \Big|_{z=0} = 0 \quad (8)$$

for  $0 \leq r \leq \ell/2$

Conditions on the lateral boundary of the plate

$$\sigma_{rr}^{(j)0} \Big|_{r=\ell/2} = -q, u_z^{(j)0} \Big|_{r=\ell/2} = 0, \text{ for } j=1,2,3; \quad (9)$$

$$\phi^{(k)0} \Big|_{r=\ell/2} = 0 \text{ for } k=1,3, \text{ under } 0 \leq z \leq 2h_F+h_C$$

This completes the full system of field equations for determination of the quantities related to the first (initial) state.

## 2.2 For the second stage

First of all, we note that in many references (see, for instance, references Guz (1981), Guz (1999) and Yang (2005), the second stage is called the perturbed state. Moreover, the field equations and relations obtained for this state are called the linearized equations and relations. Thus,

according to the monographs by Guz (1981), Guz (1999) and the monograph by Yang (2005), the linearized field equations and relations for the case under consideration are obtained as follows.

Equilibrium and electrostatic equations

$$\begin{aligned} \frac{\partial t_{rr}^{(j)}}{\partial r} + \frac{\partial t_{zz}^{(j)}}{\partial z} + \frac{1}{r}(t_{rr}^{(j)} - t_{\theta\theta}^{(j)}) &= 0 \\ \frac{\partial t_{rz}^{(j)}}{\partial r} + \frac{\partial t_{zz}^{(j)}}{\partial z} + \frac{1}{r}t_{rz}^{(j)} &= 0, \quad j=1,2,3 \\ \frac{\partial D_R^{(k)}}{\partial r} + \frac{1}{r}D_R^{(k)} + \frac{\partial D_Z^{(k)}}{\partial z} &= 0, \quad k=1,3 \end{aligned} \quad (10)$$

where

$$\begin{aligned} t_{rr}^{(j)} &= \sigma_{rr}^{(j)} + \sigma_{rr}^{(j)0} \frac{\partial u_r^{(j)}}{\partial r} \\ t_{\theta\theta}^{(j)} &= \sigma_{\theta\theta}^{(j)} + \sigma_{\theta\theta}^{(j)0} \frac{u_r^{(j)}}{r} \\ t_{zz}^{(j)} &= \sigma_{zz}^{(j)}, \quad j=1,2,3 \\ t_{rz}^{(j)} &= \sigma_{rz}^{(j)}, \quad t_{rz}^{(j)} = \sigma_{rz}^{(j)} + \sigma_{rr}^{(k)0} \frac{\partial u_z^{(j)}}{\partial r} \\ D_R^{(k)} &= D_r^{(k)} + D_r^{(k)0} \frac{\partial u_r^{(k)}}{\partial r} + \frac{\partial u_r^{(k)}}{\partial z} D_z^{(k)} \\ D_Z^{(k)} &= D_z^{(k)} + D_z^{(k)0} \frac{\partial u_z^{(k)}}{\partial z} + D_r^{(k)0} \frac{\partial u_z^{(k)}}{\partial r}, \quad k=1,3 \end{aligned} \quad (11)$$

Note that the relations in (11) are written for the case where  $\sigma_{zz}^{(j)0} = 0$  and  $\sigma_{rz}^{(j)0} = 0$  which, as will be shown below, takes place for the problem under consideration.

The electro-mechanical constitutive relations in (2), elasticity relations in (3) and the strain displacement relations in (4) also remain valid for the quantities of the second (perturbed) state. Note that under using the relations (2)-(4) for the second stage it is necessary to omit the upper index 0 in these relations. Thus, we have the complete system of field Eqs. (10), (11), (2), (3) and (4) for determination of the values related to the perturbed state.

Now we write the corresponding boundary and contact conditions.

Boundary conditions on the cracks' edges

$$\begin{aligned} t_{zr}^{(3)} \Big|_{z=h_F+h_C+0} &= 0, \quad t_{zz}^{(3)} \Big|_{z=h_F+h_C+0} = -p \\ t_{zr}^{(2)} \Big|_{z=h_F+h_C-0} &= 0, \quad t_{zz}^{(2)} \Big|_{z=h_F+h_C-0} = -p \\ t_{zr}^{(2)} \Big|_{z=h_F+0} &= 0, \quad t_{zz}^{(2)} \Big|_{z=h_F+0} = -p \end{aligned} \quad (12)$$

$$t_{zr}^{(1)} \Big|_{z=h_F-0} = 0, \quad t_{zz}^{(1)} \Big|_{z=h_F-0} = -p$$

$$D_Z^{(3)} \Big|_{z=h_F+h_C+0} = 0, \quad D_Z^{(1)} \Big|_{z=h_F-0} = 0$$

for  $0 \leq r \leq \ell_0/2$

Contact conditions between the layers in the areas which are out of the cracks

$$\begin{aligned} t_{zz}^{(3)} \Big|_{z=h_F+h_C} &= t_{zz}^{(2)} \Big|_{z=h_F+h_C} \\ t_{zr}^{(3)} \Big|_{z=h_F+h_C} &= t_{zr}^{(2)} \Big|_{z=h_F+h_C} \\ u_z^{(3)} \Big|_{z=h_F+h_C} &= u_z^{(2)} \Big|_{z=h_F+h_C} \\ u_r^{(3)} \Big|_{z=h_F+h_C} &= u_r^{(2)} \Big|_{z=h_F+h_C} \\ t_{zz}^{(2)} \Big|_{z=h_F} &= t_{zz}^{(1)} \Big|_{z=h_F}, \quad t_{zr}^{(2)} \Big|_{z=h_F} = t_{zr}^{(1)} \Big|_{z=h_F} \\ u_z^{(2)} \Big|_{z=h_F} &= u_z^{(1)} \Big|_{z=h_F}, \quad u_r^{(2)} \Big|_{z=h_F} = u_r^{(1)} \Big|_{z=h_F} \\ D_Z^{(3)} \Big|_{z=h_F+h_C} &= 0, \quad D_Z^{(1)} \Big|_{z=h_F} = 0 \quad \text{for } \ell_0/2 \leq r \leq \ell/2 \end{aligned} \quad (13)$$

Boundary conditions on the face planes of the plate

$$\begin{aligned} t_{zz}^{(3)} \Big|_{z=2h_F+h_C} &= 0, \quad t_{zr}^{(3)} \Big|_{z=2h_F+h_C} = 0, \quad t_{zz}^{(1)} \Big|_{z=0} = 0 \\ t_{zr}^{(1)} \Big|_{z=0} &= 0, \quad D_Z^{(3)} \Big|_{z=2h_F+h_C} = 0, \quad D_Z^{(1)} \Big|_{z=0} = 0 \\ &\text{for } 0 \leq r \leq \ell/2 \end{aligned} \quad (14)$$

Conditions on the lateral boundary of the plate

$$\begin{aligned} t_{rr}^{(j)} \Big|_{r=\ell/2} &= 0, \quad u_z^{(j)} \Big|_{r=\ell/2} = 0, \quad \text{for } j=1,2,3; \\ \phi^{(k)} \Big|_{r=\ell/2} &= 0 \quad \text{for } k=1,3, \quad \text{under } 0 \leq z \leq 2h_F+h_C \end{aligned} \quad (15)$$

This completes consideration of the field equations and boundary conditions related to the perturbed state and the mathematical formulation of the problem under consideration.

Now we consider the determination of the quantities related to each state.

### 3. Method of solution

We consider the determination of the sought quantities related to the initial and perturbed states separately.

#### 3.1 Determination of the values related to the

first stage (initial state)

Under determination of the initial state, according to conditions (6)-(9) and according to Saint Venant's principle, in the region where  $0 \leq r < \ell/2 - h$  the stress-strain state can be taken as homogeneous with very high accuracy. In other words, in this region we can assume that

$$\begin{aligned} \sigma_{zz}^{(k)0} = 0, \quad \sigma_{rz}^{(k)0} = 0, \quad s_{zz}^{(k)0} = 0 \\ s_{rr}^{(k)0} = s_{\theta\theta}^{(k)0} = const_k, \quad \sigma_{rr}^{(k)0} = \sigma_{\theta\theta}^{(k)0} = const_{1k} \end{aligned} \quad (16)$$

Consequently, in the initial state in the cases where  $\ell_0/2 < \ell/2 - h$  under the considered type of external loading, the existence of the cracks does not cause any stress concentration or any influence on the stress state given by the relations in (16). Taking this statement into consideration, under determination of the quantities related to the first approximation we will use the expressions given in (16).

According to the last conditions in (6)-(9), we consider the results related only to the "open-circuit" case in the planes  $z = 2h_F + h_C$ ,  $h_F + h_C$ ,  $h_F$  and  $0$ , and the "short-circuit" case on the lateral surface  $r = \ell/2$  of the plate. Therefore, in the initial state we obtain that

$$D_z^{(k)0} = D_r^{(k)0} = 0, \quad k = 1, 3 \quad (17)$$

Using the constitutive relations in (2), we obtain from (17) that

$$\begin{aligned} E_r^{(k)0} = a_1^{(k)} s_{rr}^{(k)0} + b_1^{(k)} s_{zz}^{(k)0} \\ E_z^{(k)0} = d_1^{(k)} s_{rr}^{(k)0} + c_1^{(k)} s_{zz}^{(k)0} \end{aligned} \quad (18)$$

where

$$\begin{aligned} a_1^{(k)} = \frac{\varepsilon_{13}^{(k)} (e_{31}^{(k)} + e_{32}^{(k)}) - \varepsilon_{33}^{(k)} (e_{11}^{(k)} + e_{22}^{(k)})}{\varepsilon_{11}^{(k)} \varepsilon_{33}^{(k)} - \varepsilon_{13}^{(k)} \varepsilon_{31}^{(k)}} \\ b_1^{(k)} = \frac{\varepsilon_{13}^{(k)} e_{33}^{(k)} - \varepsilon_{33}^{(k)} e_{13}^{(k)}}{\varepsilon_{11}^{(k)} \varepsilon_{33}^{(k)} - \varepsilon_{13}^{(k)} \varepsilon_{31}^{(k)}}, \quad c_1^{(k)} = \frac{\varepsilon_{11}^{(k)} e_{33}^{(k)} - \varepsilon_{31}^{(k)} e_{11}^{(k)}}{\varepsilon_{13}^{(k)} \varepsilon_{31}^{(k)} - \varepsilon_{11}^{(k)} \varepsilon_{33}^{(k)}} \\ d_1^{(k)} = \frac{\varepsilon_{11}^{(k)} (e_{31}^{(k)} + e_{32}^{(k)}) - \varepsilon_{31}^{(k)} (e_{11}^{(k)} + e_{12}^{(k)})}{\varepsilon_{13}^{(k)} \varepsilon_{31}^{(k)} - \varepsilon_{11}^{(k)} \varepsilon_{33}^{(k)}} \end{aligned} \quad (19)$$

Taking into consideration the relation  $\sigma_{zz}^{(j)0} = 0$ ,  $j = 1, 2, 3$  we obtain

$$\begin{aligned} s_{zz}^{(j)0} = a_{zr}^{(j)} s_{rr}^{(j)0} \\ a_{zr}^{(k)} = \frac{c_{31}^{(k)} + c_{32}^{(k)} - e_{13}^{(k)} a_1^{(k)} - e_{33}^{(k)} d_1^{(k)}}{c_{33}^{(k)} - e_{13}^{(k)} b_1^{(k)} - e_{33}^{(k)} c_1^{(k)}}, \quad k = 1, 3 \\ a_{zr}^{(2)} = \frac{2\lambda^{(2)}}{\lambda^{(2)} + 2\mu^{(2)}} \end{aligned} \quad (20)$$

Using the relation (20), it is obtained that

$$\begin{aligned} \sigma_{rr}^{(j)0} = A_r^{(j)} s_{rr}^{(j)0} \\ A_r^{(k)} = c_{11}^{(k)} + c_{12}^{(k)} - e_{11}^{(k)} a_1^{(k)} + a_{zr}^{(k)} c_{13}^{(k)} - \\ a_{zr}^{(k)} e_{11}^{(k)} b_1^{(k)} - a_{zr}^{(k)} e_{31}^{(k)} c_1^{(k)} \\ A_r^{(2)} = \frac{\lambda^{(2)}}{\lambda^{(2)} + 2\mu^{(2)}} \end{aligned} \quad (21)$$

Assuming that

$$s_{rr}^{(1)0} = s_{rr}^{(2)0}, \quad 2h_f \sigma_{rr}^{(1)0} + h_C \sigma_{rr}^{(2)0} = hq \quad (22)$$

The following expression is obtained for the stress in the face layers

$$\sigma_{rr}^{(1)0} = q \left( 2 \frac{h_F}{h} + \frac{h_C}{h} \frac{A_r^{(2)}}{A_r^{(1)}} \right)^{-1} \quad (23)$$

Thus, through the expressions (16)-(23) we determine completely the quantities related to the initial state. We recall that these expressions are valid for the region where  $(\ell/2 - h) \leq r < \ell/2$  and it is assumed that the materials of the face layers are the same.

3.2 Determination of the values related to the second stage (perturbed state)

For determination of the perturbed state we employ the FEM method and for this purpose, according to the monographs by Akbarov (2013), Guz (1999), Yang (2005) and others, the following functional is introduced.

$$\begin{aligned} \Pi(u_r^{(1)}, u_r^{(2)}, u_r^{(3)}, u_z^{(1)}, u_z^{(2)}, u_z^{(3)}, \phi^{(1)}, \phi^{(3)}) = \\ \frac{1}{2} 2\pi \sum_{k=1}^3 \iint_{\Omega^{(k)}} \left[ t_{rr}^{(k)} \frac{\partial u_r^{(k)}}{\partial r} + t_{\theta\theta}^{(k)} \frac{u_r^{(k)}}{r} + t_{rz}^{(k)} \frac{\partial u_z^{(k)}}{\partial r} + \right. \\ \left. t_{zr}^{(k)} \frac{\partial u_r^{(k)}}{\partial z} + t_{zz}^{(k)} \frac{\partial u_z^{(k)}}{\partial z} \right] r dr dz + \\ + \frac{1}{2} 2\pi \iint_{\Omega^{(1)}} \left[ E_r^{(1)} D_r^{(1)} + E_z^{(1)} D_z^{(1)} \right] r dr dz + \\ + \frac{1}{2} 2\pi \iint_{\Omega^{(3)}} \left[ E_r^{(3)} D_r^{(3)} + E_z^{(3)} D_z^{(3)} \right] r dr dz - \\ 2\pi \int_0^{\ell_0/2} p u_z^{(1)} \Big|_{z=h_F} r dr - 2\pi \int_0^{\ell_0/2} p u_r^{(2)} \Big|_{z=h_F} r dr - \\ 2\pi \int_0^{\ell_0/2} p u_z^{(2)} \Big|_{z=h_F+h_C} r dr - 2\pi \int_0^{\ell_0/2} p u_z^{(3)} \Big|_{z=h_F+h_C} r dr \end{aligned} \quad (24)$$

where

$$\begin{aligned}\Omega^{(1)} &= \{0 \leq r \leq \ell/2; 0 \leq z \leq h_F\} - \\ &\quad \{z = h_F - 0; 0 \leq r \leq \ell_0/2\} \\ \Omega^{(2)} &= \{0 \leq r \leq \ell/2; h_F \leq z \leq h_F + h_C\} \\ &\quad - \{z = h_F + 0; 0 \leq r \leq \ell_0/2\} \\ &\quad - \{z = h_F + h_C - 0; 0 \leq r \leq \ell_0/2\} \\ \Omega^{(3)} &= \{0 \leq r \leq \ell/2; h_F + h_C \leq z \leq 2h_F + h_C\} - \\ &\quad \{z = h_F + h_C + 0; 0 \leq r \leq \ell_0/2\}\end{aligned}\quad (25)$$

From equating to zero the first variation of the functional (24), i.e., from the relation

$$\begin{aligned}\delta\Pi &= \sum_{k=1}^3 \frac{\partial\Pi}{\partial u_r^{(k)}} \delta u_r^{(k)} + \sum_{k=1}^3 \frac{\partial\Pi}{\partial u_z^{(k)}} \delta u_z^{(k)} + \\ &\quad \frac{\partial\Pi}{\partial \phi^{(1)}} \delta \phi^{(1)} + \frac{\partial\Pi}{\partial \phi^{(3)}} \delta \phi^{(3)} = 0\end{aligned}\quad (26)$$

and after well-known mathematical manipulations we obtain the equations in (10) and all the corresponding boundary and contact conditions in (12)-(15) with respect to the forces and electrical displacements. In this way it is proven that the equations in (10) are the Euler equations for the functional (24), and the boundary and contact conditions in (12)-(15) which are given with respect to the forces and electrical displacements are the related natural boundary and contact conditions.

According to FEM modelling, the solution domains indicated in (25) are divided into a finite number of finite elements. For the considered problem, each of the finite elements is selected as a standard rectangular Lagrange family quadratic finite element (i.e., with nine nodes) and each node has three degrees of freedom, i.e., radial displacement  $u_r^{(j)}$ , transverse displacement  $u_z^{(j)}$  ( $j=1,2,3$ ) and electric potential  $\phi^{(k)}$  ( $k=1,2$ ). We note that under FEM modelling of the region containing the crack's tip, as did our predecessors, we use ordinary (not singular) finite elements. This is because up to now finite elements with oscillating singularity which appear at the interface crack tips have not been found. Furthermore, as shown in the references Akbarov (2013), Akbarov and Yahnioglu (2016), Henshell and Shaw (1975) and other ones listed therein, under calculation of the global characteristics of the element of construction (such as the critical forces, ERR, etc.) the results obtained by the use of the "ordinary" singular finite elements coincide, with very high accuracy, with the results obtained by the use of the ordinary finite elements. At the same time, the use of the singular finite elements has some inconveniencies such as no representability of the rigid-body motions and the invariability by rigid-body motion conditions which are the two main conditions required from the shape functions

under FE modelling. The algorithm and the programs to obtain the numerical results are coded within the foregoing assumptions by the authors in the FORTRAN programming language (FTN77).

Employing the standard Ritz technique detailed in many references, for instance, in the book by Zienkiewicz and Taylor (1989), we determine the displacements and electrical potential at the selected nodes. After this determination, the corresponding values of the ERR (denote it by  $\gamma$ ) are

$$\gamma = \frac{\partial U}{\pi \ell_0 \partial \ell_0} \quad (27)$$

where

$$\begin{aligned}U &= \frac{1}{2} 2\pi \sum_{k=1}^3 \iint_{\Omega^{(k)}} \left[ t_{rr}^{(k)} \frac{\partial u_r^{(k)}}{\partial r} + t_{\theta\theta}^{(k)} \frac{u_r^{(k)}}{r} + \right. \\ &\quad \left. t_{rz}^{(k)} \frac{\partial u_z^{(k)}}{\partial r} + t_{zr}^{(k)} \frac{\partial u_r^{(k)}}{\partial z} + t_{zz}^{(k)} \frac{\partial u_z^{(k)}}{\partial z} \right] r dr dz + \\ &\quad \frac{1}{2} 2\pi \iint_{\Omega^{(1)}} \left[ E_r^{(1)} D_r^{(1)} + E_z^{(1)} D_z^{(1)} \right] r dr dz + \\ &\quad \frac{1}{2} 2\pi \iint_{\Omega^{(3)}} \left[ E_r^{(3)} D_r^{(3)} + E_z^{(3)} D_z^{(3)} \right] r dr dz\end{aligned}\quad (28)$$

We recall that in (27),  $\ell_0$  is the diameter of the penny-shaped crack.

This completes the consideration of the method of solution.

## 4. Numerical results

### 4.1 The selection of the layers' materials

In the present paper, all the numerical results are made for the piezoelectric materials PZT -4, PZT -5H and BaTiO<sub>3</sub> which are selected for the face layers, however the metal materials - aluminum (Al) and steel (St) are taken as the core layer materials. The values of the elastic, piezoelectric and dielectric constants of the selected piezoelectric materials and the references used are given in Table 1. According to the monograph by Guz (2004), the values of Lamé's constants of the core layer material are selected as follows: for the Al:  $\lambda = 48.1 \text{ GPa}$  and  $\mu = 27.1 \text{ GPa}$ ; and for the St:  $\lambda = 92.6 \text{ GPa}$  and  $\mu = 77.5 \text{ GPa}$ .

In order to analyze the coupling effects of the electro-mechanical fields on the ERR, the numerical results are obtained for the following two cases

$$\text{Case 1. } e_{ij}^{(rn)} = 0, \varepsilon_{ii}^{(rn)} = 0 \quad (29)$$

Table 1 The values of the mechanical, piezoelectrical and dielectrical constants of the selected piezoelectric materials: here  $c_{11}^{(r_1)}, \dots, c_{66}^{(r_1)}$  are the elastic constants,  $e_{31}^{(r_1)}, \dots, e_{15}^{(r_1)}$  are the piezoelectric constants, and  $\varepsilon_{11}^{(r_1)}$  and  $\varepsilon_{33}^{(r_1)}$  are the dielectric constants

Mater. (Source Ref.)	$c_{11}^{(r_1)}$	$c_{12}^{(r_1)}$	$c_{13}^{(r_1)}$	$c_{33}^{(r_1)}$	$c_{44}^{(r_1)}$	$c_{66}^{(r_1)}$	$e_{31}^{(r_1)}$	$e_{33}^{(r_1)}$	$e_{15}^{(r_1)}$	$\varepsilon_{11}^{(r_1)}$	$\varepsilon_{33}^{(r_1)}$
PZT-4 (Yang 2005)	13.9	7.78	7.40	11.5	2.56	3.06	-5.2	15.1	12.7	0.646	0.562
PZT-5H (Yang 2005)	12.6	7.91	8.39	11.7	2.30	2.35	-6.5	23.3	17.0	1.505	1.302
BaTiO <sub>3</sub> (Kuna 2006)	16.6	7.66	7.75	16.2	4.29	4.29	-4.4	18.6	11.6	1.434	1.682

$\times 10^{10} N/m$ 
 $C/m^2$ 
 $\times 10^{-8} C/Vm$

$$\text{Case 2. } e_{ij}^{(r_n)} \neq 0, \varepsilon_{ii}^{(r_n)} \neq 0 \quad (30)$$

Note that the numerical results obtained in Case 1 (29) relate to the pure mechanical energies and ERR, however the numerical results obtained in Case 2 (30) relate to the total electro-mechanical energies and ERR. Comparison of the results obtained in Case 2 with the corresponding ones obtained in Case 1 will give the information for estimation of the influence of the coupling electro-mechanical effect on the studied quantities.

In the all the numerical investigations carried out in the present paper, we assume that the piezoelectric materials are polarized along the plate thickness, i.e., the polarized direction of the PZT materials coincides with the  $Oz$  axis. Moreover, all the numerical results are obtained in the case where  $h/\ell = 0.2$ .

#### 4.2 Testing of the FEM modelling and PC programs

Under FEM modelling using the symmetry with respect to the plane  $z = h_F + h_C/2$  and the axial symmetry with respect to the  $Oz$  (Fig. 1a) axis of the mechanical and geometrical properties of the plate, only the region  $\{0 \leq r \leq \ell/2; 0 \leq z \leq h_F + h_C/2\}$  is considered and this region is divided into 500 finite elements along the radial direction and 40 finite elements along the plate's thickness direction. Under fixed numbers of the finite elements, the NDOF depends on the length (or radius) of the penny-shaped crack and the NDOF increases with increasing of this length. For instance, in the case where  $\ell_0/\ell = 0.5$  we have 243499 NDOF, however, in the case where  $\ell_0/\ell = 0.3$  we have 242899 NDOF. All the corresponding PC programs are composed by the authors of the paper.

First, we consider the convergence of the numerical results with respect to the number of finite elements (FE) selected in the radial and  $Oz$  axis directions. For this purpose, consider the numerical results related to the dimensionless ERR, i.e.,  $\gamma / (c_{44}^{PZT-5H} \ell)$  for the PZT-5H/Al/PZT-5H plate. The results obtained for various values of the FE selected in the radial direction (in the  $Oz$  axis direction) are given in Table 2 (in Table 3). It follows

from these tables that the convergence of the numerical results is more sensitive with respect to the FE numbers selected in the radial direction. These and other similar results which are not given here allow us to conclude that in the convergence sense of the numerical results, it is enough to select 500 FE in the radial direction and 40 FE in the  $Oz$  axis direction in order to obtain results, the relative errors of which are less than 0.4%. Note that 40 FE in the  $Oz$  axis direction are divided in half between the face layer and half thickness of the core layer.

The foregoing convergence of the numerical results gives some confidence on the reliability of the calculation algorithm and PC programs. However, for more detailed verification of the PC programs and FEM modelling used we consider a comparison of the numerical results obtained within the scope of the present algorithm and PC programs with the corresponding ones obtained within the scope of the analytical solution method developed in the paper by Li and Lee (2012).

Table 2 Convergence of the numerical results with respect to the number of FE selected in the radial direction in the case where  $\ell_0/\ell = 0.5$ ,  $h_F/\ell = 0.05$ , and  $h_C/\ell = 0.1$  and the number of FE in the  $Oz$  axis direction is 12 for PZT-5H/Al/PZT-5H

Number of FE in the radial direct.	NDOF	$\gamma / (c_{44}^{PZT-5H} \ell)$	
		Case 1	Case 2
40	5039	5.17384	3,74138
60	7559	5.25945	3.80980
80	10079	5.31453	3.85354
100	12599	5.35750	3.88634
120	15119	5.39413	3.91292
140	17639	5.42579	3.93496
160	20159	5.45335	3.95347
200	25199	5.49826	3.98258
300	37799	5.56864	4.02635
400	50399	5.60464	4.04842
500	62999	5.62642	4.06177

Table 3 Convergence of the numerical results with respect to the number of FE selected in the  $Oz$  axis direction in the case where  $\ell_0/\ell = 0.5$ ,  $h_F/\ell = 0.05$ , and  $h_C/\ell = 0.1$  and the number of FE in the radial direction is 100 for PZT-5H/Al/PZT-5H

Number of the FE in the $Oz$ axis direc.	NDOF	$\gamma / (c_{44}^{PZT-5H} \ell)$	
		Case 1	Case 2
12	12599	5.35750	3.88634
18	18599	5.33552	3.86970
20	20599	5.33017	3.86545
24	24599	5.32377	3.85928
28	28599	5.32045	3.85535
30	39599	5.31515	3.85174
40	40599	5.30807	3.84444

We recall that the paper by Li and Lee (2012) studies an axisymmetric penny-shaped crack problem for the infinite piezoelectric layer in the case where the crack is in the middle plane of the layer and the new analytical method is developed for determination of the corresponding fundamental solutions and, by employing this method numerical, results related to the ERR are presented and discussed. Let us employ, in some particular cases, i.e. in the cases where on the crack edges the electric displacements are equal to zero and these edges are loaded with uniformly distributed mechanical opening forces with intensity  $\sigma_0$ , our FEM modelling and the PC programs for obtaining the numerical results considered in the by Li and Lee (2012). Note that under FEM modelling of the problem considered in the paper by Li and Lee (2012) we assume that  $\ell = 1m$ ,  $\ell_0 = 0.003m$  and  $h = 0.02m$ . The values selected for  $\ell_0$  and  $h$  coincide with the corresponding ones selected in the paper by Li and Lee (2012), however, the parameter  $\ell$  does not exist in the paper by Li and Lee (2012) because in that paper it is assumed that the length of the piezoelectric layer in the radial direction is infinite.

Table 4 Numerical results related to  $\gamma(N/m)$  (i.e. ERR) for the penny-shaped crack in the middle plane of the infinite PZT-5H piezoelectric layer in the case where  $\ell = 1m$ ,  $h = 0.02m$  and  $\ell_0 = 0.003m$

Sources of the results	$\sigma_0$		
	10MPa	20MPa	30MPa
Present results	3.3164	13.2655	29.8473
Results obtained in Li and Lee (2012)	3.2000	12.8000	29.4000

Thus, within the scope of the foregoing assumptions, we compare the numerical results obtained with employing of the present FEM modelling with the corresponding ones obtained in the paper by Li and Lee (2012) for the PZT-5H material. These results are given in Table 4 and it follows from the corresponding comparison that the FEM modelling and PC programs developed in the present paper are reliable enough.

### 4.3 Numerical results related to energies and energy release rate and their discussions

First we consider the case where the initial stresses in the plate-disc are absent and analyze the numerical results related to the energies. Under this analysis, the following energies in the Case 2 are distinguished:

- i) total electro-mechanical energy under calculation of which all the terms in the expression (28) are taken into consideration,
- ii) pure mechanical energy under calculation of which the last two integral terms in the expression (28) are ignored,
- iii) interaction energy under calculation of which only the terms containing the mechanical and electrical quantities simultaneously in the expression (28) are taken into consideration, and
- iv) pure electrical energy under calculation of which only the terms in the expression (28) containing only the electrical quantities are taken into consideration.

Numerical results illustrating the influence of the crack's radius on the values of the foregoing energies appearing in the PZT-5H/Al/PZT-5H and PZT-5H/St/PZT-5H plates are given in Fig. 2a and Fig. 2b, respectively. Under obtaining these results, it is assumed that  $q/c_{44}^{PZT-5H} = 0$  (i.e., the initial stresses in the layers of the plate are absent) and  $h_F/\ell = 0.025$ . It follows from these results that for all the considered lengths of the penny-shaped interface crack's radius, the values of the total electro-mechanical, pure mechanical and interaction energies are positive numbers and these values increase monotonically with this radius. However, in all the considered lengths of the crack radius, the values obtained of the pure electrical energy are negative and the absolute values of this energy also increase monotonically with the penny-shaped crack's radius. Note that in the qualitative sense, similar results are also obtained in the paper by Akbarov and Yahnioglu (2016) for the sandwich plate-strip in the plane-strain state.

The other geometrical parameter, the change of which can significantly influence the values of the energies, is the thickness of the piezoelectric face layers. As an example, this influence is illustrated by the graphs of the dependencies among the pure electrical (Fig. 3(a)), the interaction (Fig. 3(b)), the pure mechanical (Fig. 3(c)), the total electro-mechanical (Fig. 3(d)) and the dimensionless radius of the crack ( $\ell_0/\ell$ ) constructed for various

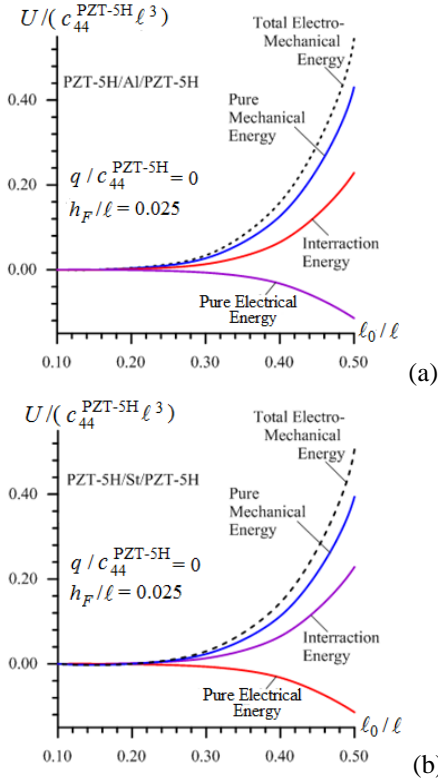


Fig. 2 Graphs of the dependencies between energies and the ratio  $\ell_0/\ell$  in Case 2 for the PZT-5H/Al/PZT-5H (a) and PZT-5H/St/PZT-5H (b) plates in the absence of initial stresses

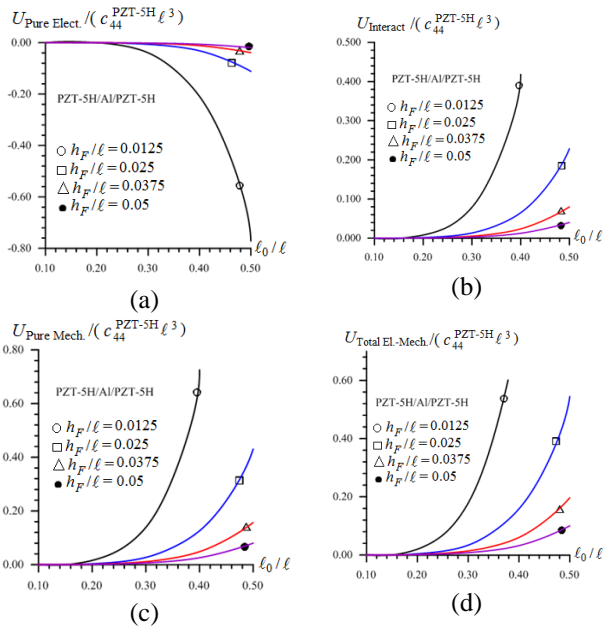


Fig. 3 Dependence of various pure electrical (a), interaction (b), pure mechanical (c) and total electro-mechanical (d) energies on the ratio  $\ell_0/\ell$  under various  $h_F/\ell$  for the PZT-5H/Al/PZT-5H plate

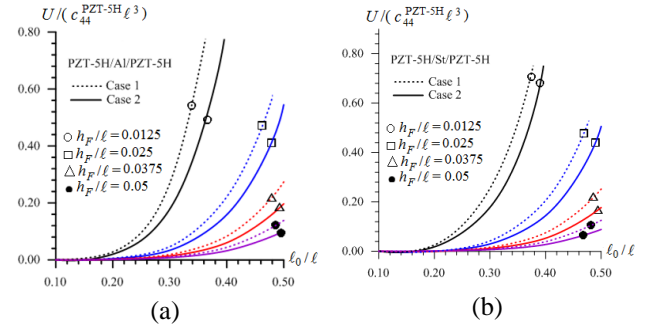


Fig. 4 The influence of the piezoelectricity of the face layers of the plates PZT-5H/Al/PZT-5H (a) and PZT-5H/St/PZT-5H (b) on the values of the total electro-mechanical energies obtained for various values of the ratios  $\ell_0/\ell$  and  $h_F/\ell$

thicknesses of the piezoelectric face layers of the PZT-5H/Al/PZT-5H plate. These results show that for a fixed thickness of the whole PZT-5H/Al/PZT-5H plate, a decrease of the face layers' thickness causes an increase in the absolute values of all the foregoing energies.

For estimation of the electro-mechanical coupling effect of the piezoelectric materials on the total electro-mechanical energy, we consider the graphs given in Fig. 4 which show the dependence between  $U$  determined by expression (28) and the dimensionless length  $\ell_0/\ell$  of the crack under various thicknesses of the face layers for PZT-5H/Al/PZT-5H (Fig. 4(a)) and PZT-5H/St/PZT-5H (Fig. 4(b)). Note that in Fig. 4, the graphs are constructed for Case 2 and Case 1 simultaneously. The difference between the corresponding results obtained in Case 1 and in Case 2 namely causes the coupling electro-mechanical effect of the piezoelectric material. We recall that, according to the expressions (28) and (29) under obtaining the results related to Case 1, the coupling effect is not taken into consideration, however, under obtaining the results related to Case 2 this effect is taken into consideration completely. Thus, it follows from the results given in Fig. 4 that for all the selected values of the layers' thickness and crack radius the piezoelectricity of the face layers' materials causes to decrease the total electro-mechanical energy of the plates under consideration.

This completes the consideration of the numerical results related to the energies. Now we consider the numerical results related to the dimensionless energy release rate (ERR) determined through the expression  $\gamma/(c_{44}^{PZT} \ell)$  and the influence of the problem parameters, as well as the influence of the initial stresses on this ERR. Under obtaining these results, the values of  $\gamma$  are calculated through the expression (27) and under this calculation the following approximate relation is used.

$$\gamma \approx \frac{\Delta U}{\pi \ell_0 \Delta \ell_0}; \quad \Delta U = U(\ell_0 + \Delta \ell_0) - U(\ell_0) \quad (31)$$

$$\Delta \ell_0/\ell = 10^{-8}$$

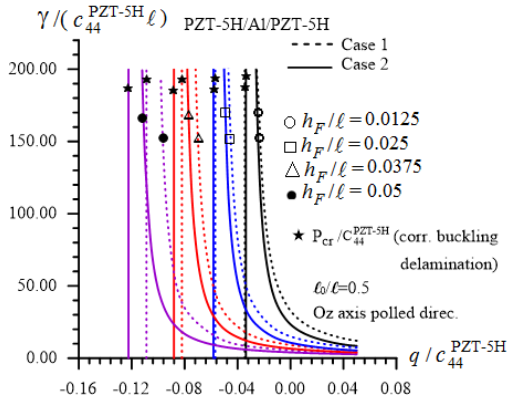


Fig. 5 Dependence between the dimensionless ERR and the initial loading obtained for the plate PZT-5H/Al/PZT-5H for various values of the ratio  $h_F/l$  under  $l_0/l = 0.5$

Note that the number  $10^{-8}$  shown in (31) for the ratio  $\Delta l_0/l$  is determined from the corresponding convergence requirement which appears for the numerical calculation of the derivative  $\partial U/\partial l_0$ .

First, we analyze the numerical results which relate to the influence of the initial stresses in the plate on the ERR and we make this analysis with respect to the PZT-5H/Al/PZT-5H plate for various  $h_F/l$  under  $l_0/l = 0.5$ . The graphs regarding these results are given in Fig. 5 from which it follows that the initial compression (stretching) of the plate layers in the inward (outward) radial direction causes an increase (a decrease) in the values of the ERR. At the same time, these results show that the ERR increases infinitely as the initial compressive forces acting in the radial inward direction approach the corresponding critical value under which buckling delamination of the plate under consideration takes place. Note that this “resonance” type phenomenon in fracture mechanics was first found by Guz for the homogeneous initially stressed elastic medium containing a crack and is detailed in the monograph by Guz (1981). For the compressed elastic layered systems with interface cracks this phenomenon is also found in the paper by Akbarov and Turan (2009). Moreover, in the paper by Akbarov and Yahnioglu (2016) this phenomenon is also found for compressed piezoelectric + elastic layered systems with interface cracks under the plane-strain state case. Consequently, the results given in Fig. 5 agree in the qualitative sense with all the corresponding results obtained earlier and these results have great significance not only in the theoretical but also the practical sense.

More detailed analysis of the results given in Fig. 5 gives us the opportunity to say that the piezoelectricity of the face layers’ materials of the plate causes the ERR to decrease and the magnitude of this “decreasing” increases with the thickness of the piezoelectric layers. Note that this and all the foregoing results on the influence of the piezoelectricity of the face layers’ materials can be explained namely with the well-known stiffening effect of the piezoelectric materials.

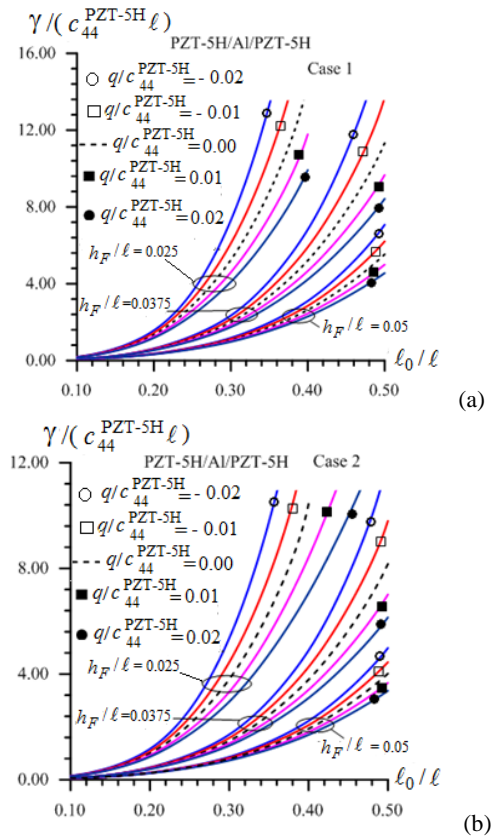


Fig. 6 The influence of the initial loading on the dependence between dimensionless ERR and crack radius for the PZT-5H/Al/PZT-5H plate in Case 1 (a) and in Case 2 (b)

Now we consider the results given in Figs. 6-8 which illustrate how an increase in the crack radius acts on the influence of the initial stresses on the ERR. Note that these results relate to the PZT-5H/Al/PZT-5H (Fig. 6), PZT-4/Al/PZT-4 (Fig. 7) and PZT-5H/St/PZT-5H (Fig. 8) plates and show the graphs between the dimensionless ERR (denoted as  $\gamma/(c_{44}^{PZT} l)$ ) and the dimensionless crack radius (denoted as  $l_0/l$ ). Note that in these figures, the graphs grouped by the letter a (by the latter b) relate to Case 1 (to Case 2).

Note that these results allow us to make a conclusion on the character of the increase of the ERR with the crack radius length. In connection with this, according to these results, it can be concluded that the dependence between the ERR and crack radius length is clearly observed to be non-linear and this nonlinearity is similar to the non-linear relation  $y = x^\lambda$  where  $\lambda > 1$ . These results also show that the initial stretching (compression) causes to decrease (to increase) the values of the ERR for all the penny-shaped crack radii and the magnitude of this decreasing (increasing) grows significantly with this radius. At the same time, according to these results, we can make some conclusions about the influence of the materials’ properties of the layers of the plate on the action of the initial stresses on the ERR. For instance, comparison of the results given in

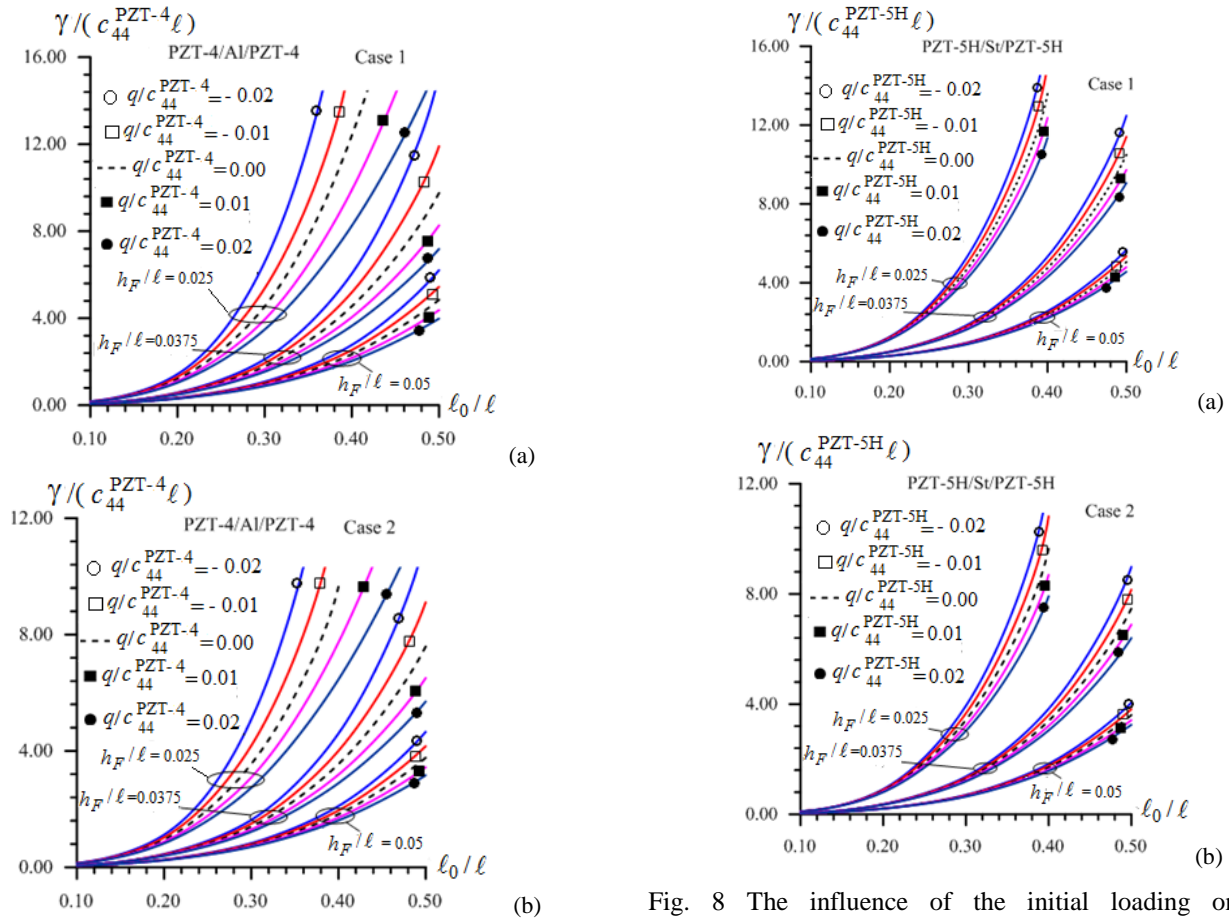


Fig. 7 The influence of the initial loading on the dependence between dimensionless ERR and crack radius for the PZT-4/Al/PZT-4 plate in Case 1 (a) and in Case 2 (b)

Fig. 8 The influence of the initial loading on the dependence between dimensionless ERR and crack radius for the PZT-5H/St/PZT-5H plate in Case 1 (a) and in Case 2 (b)

Fig. 6 with the corresponding ones given in Fig. 7 allows us to say that the difference in the results caused by the difference of the electro-mechanical properties of the considered pairs of the piezoelectric materials for the face layers, is insignificant.

However, comparison of the results given in Fig. 6 with the corresponding ones given in Fig. 8 shows that the difference which appears on account of the difference of the mechanical properties of the selected pair of materials for the core layer of the plate, is significant. In addition to all of this, comparison of the graphs given in Figs. 6, 7 and 8 and grouped by the letter a with the corresponding ones grouped by the letter b gives information on the action of the piezoelectricity of the face layers' materials on the influence of the initial stresses on the ERR. However, it is difficult to obtain a correct estimation in the quantitative sense on the action of the piezoelectricity from the comparison of these graphs and in order to make a more correct conclusion on this action in the quantitative sense, the foregoing and other additional numerical results for some discrete values of the crack radius length  $\ell_0 / \ell$  are tabulated in Tables 5-8. Note that these results relate to the PZT-5H/Al/PZT-5H (Table 5), PZT-4/Al/PZT-4 (Table 6), BaTiO<sub>3</sub>/Al/BaTiO<sub>3</sub> (Table 7)

and PZT-5H/St/PZT-5H (Table 8) plates. We recall that in these tables, the results given in the columns indicated by Case 2 (Case 1) are obtained in the case where the piezoelectricity of the face layers materials is (is not) taken into consideration, i.e. in the case where the relations in (30) (the relations in (29)) are taken into consideration.

Consequently, comparison of the results in the columns indicated by "Case 2" with the corresponding ones indicated by "Case 1" gives us correct quantitative information of the aforementioned piezoelectricity on the values of the ERR. Thus, according to this comparison we can conclude that the piezoelectricity of the face layers' materials of the plate for all the values of the geometrical parameters  $h_F / \ell$ ,  $\ell_0 / \ell$  and for all the selected pairs of plate materials decreases the values of the ERR and the magnitude of this decrease grows with the length of the penny-shaped crack radius, i.e. with  $\ell_0 / \ell$ . However, not only the magnitude of this decrease but also the magnitude of the ERR decreases with the face layers' thickness, i.e., with  $h_F / \ell$ .

Comparison of the data given in Table 5 with the corresponding ones given in Table 6 shows that the difference between them is insignificant, i.e., the results obtained for the piezoelectric PZT-5H and PZT-4 materials are close to each other.

Table 5 The values of the ERR obtained for the PZT-5H/Al/PZT-5H plate

$h_F/\ell = 0.025$										
$\ell_0/\ell$	$q/c_{44}^{PZT-5H}$									
	-0.02		-0.01		0		0.01		0.02	
	Case 1	Case 2	Case 1	Case 2	Case 1	Case 2	Case 1	Case 2	Case 1	Case 2
0.5	105.7905	79.5611	50.7413	36.6206	32.7965	23.3926	24.3000	17.2169	19.3285	13.6409
0.4	27.2848	20.0440	18.9909	13.7480	14.5351	10.4374	11.7821	8.4193	9.9202	7.0651
0.3	7.2982	5.3535	6.0969	4.4452	5.2366	3.8015	4.5923	3.3231	4.0924	2.9541
0.2	1.5691	1.1647	1.4474	1.0723	1.3438	0.9939	1.2546	0.9267	1.1770	0.8684
0.1	0.1895	0.1457	0.1843	0.1418	0.1795	0.1382	0.1750	0.1347	0.1707	0.1315
$h_F/\ell = 0.0375$										
$\ell_0/\ell$	$q/c_{44}^{PZT-5H}$									
	-0.02		-0.01		0		0.01		0.02	
	Case 1	Case 2	Case 1	Case 2	Case 1	Case 2	Case 1	Case 2	Case 1	Case 2
0.5	17.3130	12.2306	13.7086	9.7938	11.3182	8.1660	9.6629	7.0105	8.4224	6.1427
0.4	6.8152	4.8917	5.9012	4.2675	5.2053	3.7858	4.6587	3.4034	4.2186	3.0930
0.3	2.3403	1.7088	2.1538	1.5794	1.9957	1.4687	1.8600	1.3731	1.7422	1.2897
0.2	0.6276	0.4685	0.6015	0.4502	0.5777	0.4334	0.5558	0.4179	0.5356	0.4035
0.1	0.1073	0.0836	0.1055	0.0823	0.1037	0.0811	0.1020	0.0799	0.1004	0.0788
$h_F/\ell = 0.05$										
$\ell_0/\ell$	$q/c_{44}^{PZT-5H}$									
	-0.02		-0.01		0		0.01		0.02	
	Case 1	Case 2	Case 1	Case 2	Case 1	Case 2	Case 1	Case 2	Case 1	Case 2
0.5	7.0690	4.9832	6.2049	4.4483	5.5291	4.0155	4.9933	3.6633	4.5527	3.3680
0.4	3.1005	2.2265	2.8466	2.0653	2.6322	1.9265	2.4488	1.8057	2.2901	1.6997
0.3	1.1821	0.8639	1.1215	0.8249	1.0671	0.7894	1.0181	0.7570	0.9736	0.7274
0.2	0.3617	0.2699	0.3513	0.2632	0.3416	0.2568	0.3325	0.2508	0.3239	0.2452
0.1	0.0782	0.0609	0.0771	0.0602	0.0762	0.0596	0.0752	0.0590	0.0743	0.0584

However, comparison of the data given in Tables 5 and 6 with the corresponding ones given in Table 7 shows that the results obtained for the piezoelectric material BaTiO<sub>3</sub> is significantly different from those obtained for the piezoelectric materials PZT-5H and PZT-4. Note that this difference is more considerable for relatively thin face layers of the plate. At the same time, comparison of the data given in Table 5 with the corresponding ones given in Table 8 shows that the material properties of the core layer can also significantly affect the values of the ERR. For instance, in the cases under consideration the values of the ERR obtained for the plate with the St core layer are less significant than the corresponding ones obtained for the plate with the Al core layer.

Note that all the numerical results presented above and obtained in the case where the initial stresses in the plate layers are absent, i.e., in the case where  $p/c_{44}^{PZT} = 0$ , are also new ones and all conclusions given above on the influence of the problem parameters (except the parameter regarding the initial stresses) on the energies and the ERR also relate to this case.

With this we restrict ourselves to consideration and discussion of the numerical results.

## 5. Conclusions

Thus, in the present paper, the interface penny-shaped crack problem for the initially rotationally symmetric compressed (or stretched) in the inward (outward) radial direction PZT/Elastic/PZT sandwich circular plate is considered by utilizing the so-called three-dimensional linearized field equations and relations of the electro-elasticity for piezoelectric materials. The quantities related to the initial stress state are determined within the scope of the classical linear theory of piezoelectricity. Under this determination, within the framework of certain restrictions, the existence of the interface cracks is not taken into consideration. However, the corresponding mathematical problem formulation and determination of the quantities related to the perturbed state, i.e., for the state which appears as a result of the action of the uniformly normal

Table 6 The values of the ERR obtained for the PZT-4/Al/PZT-4 plate

$h_F/\ell = 0.025$										
$q/c_{44}^{PZT-4}$										
$\ell_0/\ell$	-0.02		-0.01		0		0.01		0.02	
	Case 1	Case 2	Case 1	Case 2	Case 1	Case 2	Case 1	Case 2	Case 1	Case 2
0.5	105.6929	78.6906	44.5352	34.2548	27.7275	21.4948	20.1143	15.6678	15.8351	12.3461
0.4	25.0674	19.1414	16.6265	12.8488	12.4053	9.6434	9.9027	7.7255	8.2549	6.4547
0.3	6.5821	5.0821	5.3779	4.1787	4.5480	3.5492	3.9435	3.0872	3.4843	2.7344
0.2	1.4345	1.1174	1.3092	1.0242	1.2048	0.9459	1.1165	0.8792	1.0409	0.8218
0.1	0.1834	0.1451	0.1776	0.1410	0.1723	0.1372	0.1673	0.1336	0.1626	0.1302
$h_F/\ell = 0.0375$										
$q/c_{44}^{PZT-4}$										
$\ell_0/\ell$	-0.02		-0.01		0		0.01		0.02	
	Case 1	Case 2	Case 1	Case 2	Case 1	Case 2	Case 1	Case 2	Case 1	Case 2
0.5	15.2707	11.3989	11.9062	9.1072	9.7594	7.5867	8.2697	6.5021	7.1848	5.6959
0.4	6.0548	4.5972	5.1945	4.0026	4.5505	3.5454	4.0511	3.1838	3.6531	2.8909
0.3	2.1166	1.6258	1.9356	1.5004	1.7841	1.3936	1.6554	1.3015	1.5448	1.2214
0.2	0.5872	0.4555	0.5604	0.4373	0.5362	0.4206	0.5141	0.4052	0.4940	0.3911
0.1	0.1069	0.0848	0.1048	0.0835	0.1028	0.0822	0.1010	0.0810	0.0992	0.0798
$h_F/\ell = 0.05$										
$q/c_{44}^{PZT-4}$										
$\ell_0/\ell$	-0.02		-0.01		0		0.01		0.02	
	Case 1	Case 2	Case 1	Case 2	Case 1	Case 2	Case 1	Case 2	Case 1	Case 2
0.5	6.2121	4.6543	5.4455	4.1613	4.8513	3.7638	4.3739	3.4362	3.9856	3.1632
0.4	2.7757	2.1034	2.5432	1.9527	2.3476	1.8226	2.1809	1.7094	2.0372	1.6099
0.3	1.0852	0.8287	1.0273	0.7914	0.9756	0.7576	0.9292	0.7266	0.8873	0.6983
0.2	0.3448	0.2650	0.3343	0.2585	0.3245	0.2522	0.3153	0.2464	0.3067	0.2408
0.1	0.0788	0.0622	0.0777	0.0616	0.0766	0.0609	0.0756	0.0603	0.0746	0.0597

opening forces acting on the penny-shaped crack's edges are determined with the use of the three-dimensional linearized equations and relations of piezoelectricity. The values related to the initial stress state are determined analytically, however, the values related to the perturbed state are determined numerically by employing FEM.

For obtaining numerical results on the energies and ERR caused by the aforementioned additional opening forces, the corresponding algorithm and PC programs are composed and tested with the corresponding known results. Numerical results are presented and discussed for the PZT-5H/Al/PZT-5H, PZT-4/Al/PZT-4, BaTiO<sub>3</sub>/Al/BaTiO<sub>3</sub> and PZT-5H/St/PZT-5H sandwich plates. According to analyses of the results, the following concrete conclusions can be made:

- The piezoelectricity of the face layers' materials causes to decrease the total electro-mechanical energies and the magnitude of this influence increases with increasing of the ratio  $\ell_0/\ell$  and with decreasing of the ratio  $h_F/\ell$ , where  $\ell_0/2$  ( $\ell/2$ ) is the radius of the penny-shaped crack (circular disc),

and  $h_F$  is the thickness of the piezoelectric face layer.

Consequently, the parameters  $\ell_0/\ell$  and  $h_F/\ell$  characterize not only the dimensions of the penny-shaped crack and face layer thickness, but also the dimension of the circular plate;

- Initial compressing (stretching) of the plate-disc in the inward (outward) radial direction causes an increase (a decrease) in the values of the ERR: in the initial compression case the values of the ERR increase indefinitely as the compressive force approaches the critical values of those determined in the paper by Cafarova *et al.* (2017) and the corresponding buckling delamination of the plates under consideration;
- The piezoelectricity of the face layers' materials causes to decrease the values of the ERR;
- The values of the ERR increase (decrease) with the ratio  $\ell_0/\ell$  (with the ratio  $h_F/\ell$ );

The magnitude of the ERR depends not only on the electro-mechanical properties of the face layers' materials, but also on the mechanical properties of the elastic core layer.

Table 7 The values of the ERR obtained for the BaTiO<sub>3</sub>/Al/BaTiO<sub>3</sub> plate

$h_F/\ell = 0.025$										
$q/c_{44}^{BaTiO_3}$										
$\ell_0/\ell$	-0.02		-0.01		0		0.01		0.02	
	Case 1	Case 2	Case 1	Case 2	Case 1	Case 2	Case 1	Case 2	Case 1	Case 2
0.5	2417.3837	2025.1235	76.5139	71.4054	33.7653	31.6862	21.6628	20.3676	16.0531	15.0881
0.4	57.7433	53.5387	24.3820	22.8322	15.1945	14.2689	11.0537	10.3936	8.7196	8.2048
0.3	10.3557	9.6798	7.2818	6.8317	5.6139	5.2771	4.5764	4.3070	3.8714	3.6465
0.2	1.9755	1.8528	1.7093	1.6064	1.5085	1.4200	1.3519	1.2741	1.2264	1.1570
0.1	0.2439	0.2297	0.2328	0.2195	0.2228	0.2104	0.2138	0.2021	0.2056	0.1945
$h_F/\ell = 0.0375$										
$q/c_{44}^{BaTiO_3}$										
$\ell_0/\ell$	-0.02		-0.01		0		0.01		0.02	
	Case 1	Case 2	Case 1	Case 2	Case 1	Case 2	Case 1	Case 2	Case 1	Case 2
0.5	24.4564	22.4742	16.1063	15.0065	11.9706	11.2406	9.5450	8.9976	7.9494	7.5171
0.4	8.66798	8.0449	6.8134	6.3707	5.6159	5.2759	4.7824	4.5079	4.1707	3.9406
0.3	2.85373	2.6623	2.4962	2.3386	2.2206	2.0872	2.0020	1.8865	1.8245	1.7227
0.2	0.77068	0.7213	0.7208	0.6764	0.6775	0.6372	0.6396	0.6027	0.6062	0.5722
0.1	0.14166	0.1333	0.1380	0.1301	0.1345	0.1271	0.1313	0.1242	0.1283	0.1215
$h_F/\ell = 0.05$										
$q/c_{44}^{BaTiO_3}$										
$\ell_0/\ell$	-0.02		-0.01		0		0.01		0.02	
	Case 1	Case 2	Case 1	Case 2	Case 1	Case 2	Case 1	Case 2	Case 1	Case 2
0.5	8.4975	7.8539	7.0066	6.5346	5.9660	5.5976	5.2005	4.9025	4.6113	4.3619
0.4	3.6698	3.4083	3.2404	3.0266	2.9030	2.7237	2.6313	2.4776	2.4081	2.2740
0.3	1.4063	1.3099	1.3034	1.2186	1.2154	1.1399	1.1392	1.0713	1.0727	1.0111
0.2	0.4439	0.4143	0.4259	0.3984	0.4094	0.3838	0.3944	0.3704	0.3806	0.3581
0.1	0.1036	0.0973	0.1017	0.0957	0.1000	0.0942	0.0983	0.0927	0.0967	0.0913

For instance, the values of the ERR obtained for the plate with the St core layer are significantly less than the corresponding ones obtained for the same plate with the Al core layer;

- Numerical results obtained in the present paper in the qualitative sense agree with the corresponding ones obtained in related investigations carried out, for instance, in the papers by Yang (2004), McMeeking and Landis (2008), Li and Lee (2012), Akbarov and Yahnioglu (2016), Akbarov and Turan (2009) and others.

## References

- Akbarov, S.D. (2013), *Stability Loss and Buckling Delamination: Three-Dimensional Linearized Approach for Elastic and Viscoelastic Composites*, Springer, Heidelberg, New York, USA.
- Akbarov, S.D. and Yahnioglu, N. (2013), "Buckling delamination of a sandwich plate-strip with piezoelectric face and elastic core layers", *Appl. Math. Model.*, **37**, 8029-8038.
- Akbarov, S.D. and Yahnioglu, N. (2016), "On the total electro-mechanical potential energy and energy release rate at the interface crack tips in an initially stressed sandwich plate-strip with piezoelectric face and elastic core layers", *Int. J. Solids Struct.*, **88-89**, 119-130.
- Akbarov, S.D. and Turan, A. (2009), "Mathematical modelling and the study of the influence of initial stresses on the SIF and ERR at the crack tips in a plate-strip of orthotropic material", *Appl. Math. Model.*, **33**, 3682-3692.
- Cafarova, F.I., Akbarov, S.D. and Yahnioglu, N. (2017), "Buckling delamination of the PZT/Metal/PZT sandwich circular plate-disc with penny-shaped interface cracks", *Smart Struct. Syst.*, **19**(2), 163-179.
- Feng W.J., Li, Y.S. and Xu, Z.H. (2009), "Transient response of an interfacial crack between dissimilar magneto-electroelastic layers under magneto-electro-mechanical impact loadings: Mode -I problem", *Int. J. Solids Struct.*, **46**, 3346-3356.
- Eskandari, M., Moeini-Ardakani, S.S. and Shodja, H.M. (2010), "An energetically consistent annular crack in a piezoelectric medium", *Eng. Fract. Mech.*, **77**, 819-831.
- Guz, A.N. (1981), *Brittle Fracture of the Materials with Initial Stresses*, Naukova Dumka, Kiev, Ukraine (in Russian).

Table 8 The values of the ERR obtained for the PZT-5H/St/PZT-5H plate

$h_F/\ell = 0.025$										
$\ell_0/\ell$	$q/c_{44}^{PZT-5H}$									
	-0.02		-0.01		0		0.01		0.02	
	Case 1	Case 2	Case 1	Case 2	Case 1	Case 2	Case 1	Case 2	Case 1	Case 2
0.5	44.1525	32.6636	36.4882	26.2783	31.0229	21.9283	27.0238	18.8883	23.9477	16.5414
0.4	16.9125	12.3249	15.0664	10.8169	13.5833	9.6376	12.3676	8.6912	11.3550	7.9157
0.3	5.4398	3.9387	5.0989	3.6636	4.7989	3.4247	4.5325	3.2155	4.2940	3.0308
0.2	1.2612	0.9139	1.2224	0.8828	1.1861	0.8538	1.1519	0.8268	1.1196	0.8014
0.1	0.1479	0.1081	0.1463	0.1068	0.1447	0.1056	0.1431	0.1043	0.1416	0.1031
$h_F/\ell = 0.0375$										
$\ell_0/\ell$	$q/c_{44}^{PZT-5H}$									
	-0.02		-0.01		0		0.01		0.02	
	Case 1	Case 2	Case 1	Case 2	Case 1	Case 2	Case 1	Case 2	Case 1	Case 2
0.5	12.4745	8.9804	11.4059	8.1531	10.4923	7.4647	9.7264	6.8877	9.0634	6.3977
0.4	5.3217	3.8296	5.0196	3.5980	4.7502	3.3932	4.5089	3.2107	4.2915	3.0471
0.3	1.9041	1.3728	1.8385	1.3226	1.7773	1.2760	1.7202	1.2327	1.6668	1.1923
0.2	0.5105	0.3694	0.5011	0.3623	0.4921	0.3555	0.4835	0.3489	0.4751	0.3426
0.1	0.0814	0.0594	0.0807	0.0589	0.0801	0.0585	0.0795	0.0580	0.0789	0.0576
$h_F/\ell = 0.05$										
$\ell_0/\ell$	$q/c_{44}^{PZT-5H}$									
	-0.02		-0.01		0		0.01		0.02	
	Case 1	Case 2	Case 1	Case 2	Case 1	Case 2	Case 1	Case 2	Case 1	Case 2
0.5	5.6705	4.0507	5.3429	3.8132	5.0496	3.6037	4.7909	3.4167	4.5571	3.2492
0.4	2.5567	1.8310	2.4562	1.7586	2.3636	1.6918	2.2779	1.6300	2.1984	1.5728
0.3	0.9819	0.7049	0.9575	0.6874	0.9343	0.6707	0.9123	0.6549	0.8913	0.6398
0.2	0.2947	0.2119	0.2906	0.2089	0.2866	0.2061	0.2827	0.2033	0.2789	0.2006
0.1	0.0591	0.0428	0.0587	0.0426	0.0583	0.0423	0.0579	0.0420	0.0575	0.0418

- Guz, A.N. (1999), *Fundamentals of the Three-Dimensional Theory of Stability of Deformable Bodies*, Springer-Verlag, Berlin, Heidelberg, Germany.
- Guz, A.N. (2004), *Elastic Waves in Bodies With Initial (Residual) Stresses*, "A.C.K.", Kiev, Ukraine.
- Henshell, R.D. and Shaw, K.G. (1975), "Crack tip finite elements are unnecessary", *Int. J. Numer. Meth. Eng.*, **9**, 495-507.
- Kuna, M. (2006), "Finite element analysis of cracks in piezoelectric structures: a survey", *Arch. Appl. Mech.*, **76**, 725-745.
- Kuna, M. (2010), "Fracture mechanics of piezoelectric materials – where are we right now?", *Eng. Fract. Mech.*, **77**, 309-326.
- Kudryatsev, B.A., Parton, V.Z. and Rakin, V.I. (1975), "Breakdown mechanics of piezoelectric materials – axisymmetric crack on boundary with conductor", *Prikl. Math. Mekh.*, **39**, 352 – 362.
- Landis, C.M. (2004), "Energetically consistent boundary conditions for electro-mechanical fracture", *Int. J. Solids Struct.*, **41**, 6291-6315.
- Li, Y.D. and Lee, K.Y. (2012), "Three dimensional axisymmetric problems in piezoelectric media: Revisited by a real fundamental solutions based new method", *Appl. Math. Model.*, **36**, 6100-6113.
- Li, Y.S., Cai, Z.Y. and Wang, W. (2011), "Electroelastic behaviour of annular interfacial crack between dissimilar crack between dissimilar piezoelectric layers", *Philos. Mag.*, **91**(23), 3155-3172.
- Li, Y.S., Feng, W.J. and Xu, Z.H. (2009), "A penny-shaped interface crack between a functionally graded piezoelectric layer and a homogeneous piezoelectric layer", *Mechanica*, **44**(4) 377-387.
- Li, W., McMeeking, R.M. and Landis, C.M. (2008), "On the crack face boundary conditions in electro-mechanical fracture and an experimental protocol for determining energy release rates", *Eur. J. Mech. A - Solids*, **27**, 285-301.
- Narita, F., Lin, S. and Shindo, Y. (2003), "Penny-shaped crack in a piezoelectric cylinder under Mode I loading", *Arch. Mech.*, **55**(3), 275-304.
- Parton, V.Z. (1976), "Fracture mechanics of piezoelectric materials", *Acta Astronaut.*, **3**(9-10), 671-683.
- Ren, J.N., Li, Y.S. and Wang, W. (2014), "A penny-shaped interfacial crack between piezoelectric layer and elastic half-space", *Struct. Eng. Mech.*, **62**(1), 1-17.
- Yang, F. (2004), "General solutions of a penny-shaped crack in a piezoelectric material under opening mode loading", *Q. J. Mech. Appl. Math.*, **57**(4), 529-550.

- Yang, J. (2005), *An Introduction to the Theory of Piezoelectricity*, Springer, New York, USA.
- Zienkiewicz, O.C. and Taylor, R.L. (1989), *The Finite Element Method: Basic Formulation and Linear Problems*. Vol. 1., Fourth Ed., McGraw-Hill Book Company, Oxford, UK.
- Zhong, X.C. (2012), "Fracture analysis of a piezoelectric layer with a penny-shaped and energetically consistent crack", *Acta Mech.*, **223**, 331-345.

HJ